

Contribution from the Department of Chemistry, University of British Columbia,  
Vancouver, British Columbia V6T 1W5, Canada

## Crystal and Molecular Structure of (5,10,15,20-Tetraphenylporphinato)indium(III) Chloride<sup>1a</sup>

R. G. BALL,\* K. M. LEE, A. G. MARSHALL,<sup>1b</sup> and J. TROTTER

Received November 29, 1979

The first crystal and molecular structure of an indium porphyrin has been determined by X-ray diffraction. (5,10,15,20-Tetraphenylporphinato)indium(III) chloride crystallized in the space group  $P2_1/n$ , with unit cell dimensions of  $a = 10.099$  (1) Å,  $b = 16.117$  (2) Å,  $c = 21.090$  (2) Å,  $\beta = 90.70^\circ$ , and four molecules per unit cell. The structure was solved by using heavy-atom methods and refined by full-matrix least-squares techniques on  $F$ , using 5096 independent reflections having  $F^2 > 3\sigma(F^2)$ , to final agreement factors of  $R_1 = 0.047$  and  $R_2 = 0.064$ . The indium is five-coordinate in a square-pyramidal complex with chloride as the axial ligand. The average In-N bond length is 2.156 (6) Å, with an In-Cl distance of 2.369 (2) Å. The porphinato core is somewhat expanded with an average radius of 2.067 (3) Å, and the macrocycle is nonplanar with some net doming toward the indium. The indium atom is located 0.61 Å above the mean plane of the four pyrrole nitrogens. Inequivalence of the phenyl tilt angles is explained by crystal packing; all four phenyls are equivalent in solution. Reconstitution of indium porphyrins into apomyoglobin and apohemoglobin is proposed.

### Introduction

According to the most recent published compilation,<sup>2</sup> the crystal and molecular structures of more than 120 porphyrins and metalloporphyrins had been determined by X-ray diffraction by 1976. A major reason for this high and continuing interest in the bond lengths, metal disposition, and distortions in the porphyrin core structure of metalloporphyrins is that pronounced variations in these parameters occur on oxygen binding to myoglobin and hemoglobin and are proposed to relate directly to the cooperative oxygen-binding function of hemoglobin.<sup>3</sup> Although at least 20 metalloporphyrin complexes exhibit structures with the metal atom displaced by varying distances above the mean plane of the four pyrrole nitrogens of the porphyrin skeleton, virtually none fulfill the useful requirements (see below) that the metal displacement be similar to that in hemoglobin and that the metal be stable to oxidation. Since In(III) is oxidation stable in aqueous solution and has an ionic radius similar to that of Fe(II), we decided to determine the crystal and molecular structure of an indium porphyrin complex. The results (see below) suggest that reconstitution of myoglobin or hemoglobin with indium porphyrins should provide information of direct relevance to proposed models for hemoglobin function.

### Experimental Section

Indium chloride (anhydrous, ultrapure) was obtained from Alfa; meso-tetraphenylporphine (TPP) was obtained from Strem Chemicals, Inc. The procedure used to synthesize the indium meso-tetraphenylporphyrin chloride was essentially that of Bhatti et al.<sup>4</sup> However, in this case the crude product was purified by chromatography on silica gel in toluene solution. The InTPP-Cl was eluted with toluene/methanol (1:1).

Recrystallization was carried out by dissolving the metalloporphyrin in a minimal amount of chloroform and adding methanol dropwise to the boiling solution. With continued boiling, chloroform distilled away, and the methanol concentration increased; this process was allowed to continue until some small crystals formed. Purple single crystals were obtained by letting the mixture stand for several days at room temperature.

Table I. Crystal Data and Conditions for Data Collection

$C_{44}H_{28}ClInN_4$	fw = 763.015
space group $P2_1/n$	vol = 3432.5 Å <sup>3</sup>
$a = 10.099$ (1) Å	$Z = 4$
$b = 16.117$ (2) Å	$D_c = 1.476$ g cm <sup>-3</sup>
$c = 21.090$ (2) Å	$D_o^a = 1.48$ (1) g cm <sup>-3</sup>
$\beta = 90.70$ (1) <sup>o</sup>	$\mu = 7.22$ cm <sup>-1</sup>

radiation: Mo K $\alpha$ , graphite monochromator  
 scan type:  $\omega$ -2 $\theta$   
 scan range:  $(0.47 + 0.35 \tan \theta)^\circ$  in  $\omega$ , extended 25% for each background measurement  
 scan speed: 0.75-10.1<sup>o</sup> min<sup>-1</sup>, to give  $I/\sigma(I) \geq 20$   
 aperture: 1.33 × 4 mm, 173 mm from crystal  
 standards: 190, 641, 0, 5, T2, 604; measured every hour of exposure time  
 data collected:  $\pm h, k, l$  for  $2\theta \leq 55^\circ$ ; 7859 reflections  
 $\sigma(I)$ :  $\{Int + 4(BG) + (0.04I)^2\}^{1/2}$ ; Int is integrated peak count, BG is the sum of the background counts, and  $I$  is the intensity

<sup>a</sup> By neutral buoyancy in CCl<sub>4</sub> and CH<sub>2</sub>Cl<sub>2</sub>.

**Collection and Reduction of X-ray Intensity Data.** Preliminary precession photographs showed the crystals to be monoclinic with systematic absences,  $k$  odd for  $0k0$  and  $h + l$  odd for  $h0l$ , which unambiguously determine the space group to be  $P2_1/n$ , an alternative setting of  $P2_1/c$ , with equivalent positions,  $\pm(x, y, z; 1/2 + x, 1/2 - y, 1/2 + z)$ .

The crystal chosen for data collection was of approximate dimensions, 0.28 × 0.25 × 0.13 mm, with eight faces of the forms {101} and {012}. It was mounted in a nonspecific orientation on an Enraf-Nonius CAD-4 diffractometer, and the cell constants and orientation matrix were determined from a least-squares fit to 25 reflections having  $23^\circ < 2\theta < 34^\circ$ . The crystal data and experimental conditions for data collection are given in Table I.

A total of 7859 independent reflections, excluding those systematically absent, was measured and processed.<sup>5</sup> Of these, 5096 had  $F^2 > 3\sigma(F^2)$  and were used in the structure solution and refinement.

**Structure Solution and Refinement.** The positional parameters for the In and Cl atoms were determined from a three-dimensional Patterson synthesis, and the remaining nonhydrogen atoms were found by the usual combination of least-squares refinement and difference Fourier syntheses.

Refinement of atomic parameters was carried out by using full-matrix least-squares techniques on  $F$  and minimizing the function  $\sum w(|F_o| - |F_c|)^2$ , where  $|F_o|$  and  $|F_c|$  are the observed and calculated structure factor amplitudes and the weighting factor  $w$  is given by

- (1) (a) This work was supported by grants from the Natural Sciences and Engineering Research Council of Canada (A.G.M., Grant No. A-6178; J.T., Grant No. A-1121), the University of British Columbia (A.G.M.; J.T.), and the Alfred P. Sloan Foundation (A.G.M.). (b) Alfred P. Sloan Research Fellow, 1976-1980.
- (2) J. Trotter, Ed., "Structure Reports", Vol. 1-42, Bohn, Scheltema & Holkema, Utrecht, 1978.
- (3) M. F. Perutz, *Sci. Am.*, **239**, 92-125 (1978).
- (4) M. Bhatti, W. Bhatti, and E. Mast, *Inorg. Nucl. Chem. Lett.*, **8**, 133-7 (1972).

- (5) The computer programs used include locally written programs for data processing and locally modified versions of the following: ORFLS, full-matrix least squares, and ORFFE, function and errors, by W. R. Busing, K. O. Martin, and H. A. Levy; Patterson and Fourier synthesis, FORDAP, by A. Zalkin; crystal structure illustrations, ORTEP II, by C. K. Johnson.

Table II. Final Atomic Positional and Thermal Parameters<sup>a</sup>

atom	x	y	z	$U_{11}^b$	$U_{22}$	$U_{33}$	$U_{12}$	$U_{13}$	$U_{23}$
In	3493.1 (3)	1797.0 (2)	1516.3 (1)	4.23 (2)	3.34 (2)	2.64 (2)	-0.39 (2)	-0.33 (1)	0.20 (1)
Cl	1387 (1)	2388 (1)	1706 (1)	5.2 (1)	6.1 (1)	5.5 (1)	0.8 (1)	-0.1 (1)	-0.5 (1)
N(1)	3284 (4)	499 (3)	1749 (2)	5.6 (2)	3.4 (2)	3.0 (2)	-0.4 (2)	-0.3 (2)	0.2 (2)
N(4)	3522 (4)	1389 (3)	548 (2)	5.5 (3)	3.5 (2)	2.8 (2)	-0.3 (2)	-0.3 (2)	0.0 (2)
N(3)	4761 (4)	2789 (3)	1202 (2)	5.1 (2)	4.0 (2)	3.1 (2)	-0.7 (2)	-0.3 (2)	0.2 (2)
N(2)	4579 (4)	1891 (3)	2401 (2)	4.6 (2)	3.8 (2)	3.1 (2)	-0.8 (2)	-0.6 (2)	0.5 (2)
C(1)	2844 (5)	-119 (3)	1341 (2)	4.8 (3)	3.4 (3)	4.1 (3)	-0.5 (2)	-0.3 (2)	-0.0 (2)
C(2)	2665 (6)	-863 (3)	1703 (3)	6.9 (4)	3.7 (3)	4.6 (3)	-1.0 (3)	-0.8 (3)	0.6 (2)
C(3)	3018 (6)	-703 (3)	2310 (3)	7.0 (4)	4.1 (3)	4.0 (3)	-0.8 (3)	-0.8 (3)	1.0 (2)
C(4)	3395 (5)	150 (3)	2346 (2)	5.2 (3)	3.7 (3)	3.2 (2)	-0.2 (2)	-0.4 (2)	0.5 (2)
C(5)	3909 (5)	560 (3)	2886 (2)	4.5 (3)	3.9 (3)	3.6 (2)	-0.6 (2)	-0.2 (2)	0.7 (2)
C(6)	4445 (5)	1361 (3)	2909 (2)	5.0 (3)	4.1 (3)	3.1 (2)	-0.6 (2)	-0.4 (2)	0.6 (2)
C(7)	4976 (6)	1760 (4)	3462 (2)	6.7 (3)	5.1 (3)	3.1 (2)	-0.9 (3)	-1.0 (2)	0.9 (2)
C(8)	5423 (5)	2510 (4)	3286 (2)	5.8 (3)	5.5 (3)	3.5 (3)	-1.4 (3)	-0.9 (2)	0.4 (2)
C(9)	5199 (5)	2601 (3)	2619 (2)	4.3 (3)	4.6 (3)	3.2 (2)	-0.6 (2)	-0.7 (2)	0.2 (2)
C(10)	5581 (5)	327.7 (3)	2247 (2)	4.7 (3)	4.5 (3)	3.5 (2)	-0.7 (2)	-0.7 (2)	0.4 (2)
C(11)	5392 (5)	3358 (3)	1590 (2)	4.9 (3)	4.4 (3)	3.7 (2)	-1.2 (2)	-0.5 (2)	0.4 (2)
C(12)	5890 (6)	4024 (4)	1207 (2)	6.5 (4)	5.1 (3)	4.1 (3)	-2.2 (3)	-0.7 (2)	0.6 (3)
C(13)	5575 (6)	3846 (4)	597 (2)	6.1 (3)	5.2 (3)	3.9 (3)	-2.0 (3)	-0.1 (2)	0.9 (2)
C(14)	4856 (5)	3077 (3)	589 (2)	4.7 (3)	4.0 (3)	3.1 (2)	-0.4 (2)	0.0 (2)	0.9 (2)
C(15)	4393 (5)	2667 (3)	48 (2)	4.7 (3)	4.3 (3)	3.1 (2)	-0.3 (2)	0.1 (2)	0.4 (2)
C(16)	3783 (5)	1885 (3)	33 (2)	4.9 (3)	4.0 (3)	3.1 (2)	0.1 (2)	0.0 (2)	0.4 (2)
C(17)	3390 (6)	1450 (4)	-534 (2)	6.9 (4)	4.9 (3)	2.9 (2)	-0.1 (3)	-0.1 (2)	0.3 (2)
C(18)	2896 (6)	711 (3)	-358 (2)	6.4 (3)	4.1 (3)	3.1 (2)	-0.7 (2)	-0.5 (2)	-0.4 (2)
C(19)	2988 (5)	663 (3)	321 (2)	5.0 (3)	3.9 (3)	3.1 (2)	-0.2 (2)	-0.3 (2)	-0.4 (2)
C(20)	2665 (5)	-40 (3)	688 (2)	4.7 (3)	3.9 (3)	3.6 (2)	-0.4 (2)	-0.3 (2)	-0.7 (2)

<sup>a</sup> Estimated standard deviations in this and other tables are given in parentheses and correspond to the least significant digits. The positional parameters have been multiplied by  $10^4$  and the thermal parameters by  $10^2$ . <sup>b</sup>  $U_{ij} = \beta_{ij}/(2\pi^2 a_i^* a_j^*) \text{ \AA}^2$ . The thermal ellipsoid is given by  $\exp[-(\beta_{11}h^2 + \beta_{22}k^2 + \beta_{33}l^2 + 2\beta_{12}hk + 2\beta_{13}hl + 2\beta_{23}kl)]$ .

Table III. Rigid Group Parameters

group	$x_c^a$	$y_c$	$z_c$	$\delta$	$\epsilon$	$\eta$
1C1-1C6	0.1566 (2)	-0.1402 (2)	-0.0041 (1)	1.430 (3)	-2.662 (2)	0.666 (3)
2C1-2C6	0.4074 (3)	-0.0409 (2)	0.4037 (1)	-1.642 (3)	3.017 (2)	-2.137 (3)
3C1-3C6	0.7040 (3)	0.4590 (2)	0.2875 (1)	-2.114 (3)	2.997 (3)	-0.457 (3)
4C1-4C6	0.4835 (3)	0.3297 (2)	-0.1213 (1)	-1.899 (3)	-3.100 (2)	1.245 (3)

group	$B_1^b$	$B_2$	$B_3$	$B_4$	$B_5$	$B_6$
1C1-1C6	3.38 (9)	4.5 (1)	5.3 (1)	4.8 (1)	4.7 (1)	4.1 (1)
2C1-2C6	3.38 (9)	4.6 (1)	5.1 (1)	5.1 (1)	5.0 (1)	4.3 (1)
3C1-3C6	3.37 (9)	4.3 (1)	4.9 (1)	5.2 (1)	5.6 (1)	4.7 (1)
4C1-4C6	3.7 (1)	5.2 (1)	6.3 (2)	6.2 (2)	6.3 (2)	5.5 (1)

<sup>a</sup> See S. J. LaPlace and J. A. Ibers, *Acta Crystallogr.*, 18, 511 (1965), for definition of group parameters. <sup>b</sup>  $B_n$  is the temperature factor of atom  $C_n$  in the phenyl ring in  $\text{\AA}^2$ .

$w = 4F_o^2/\sigma^2(F_o^2)$ . The neutral atom scattering factors for all atoms were calculated from the analytical expression for the scattering factor curves.<sup>6a</sup> The  $f'$  and  $f''$  components of anomalous dispersion were those of Cromer and Liberman<sup>6b</sup> and were included in the calculations for the In and Cl atoms.

Two cycles of least-squares refinement, with the In and Cl atoms assigned anisotropic temperature factors, with the atoms of the four phenyl rings constrained as rigid groups ( $D_{6h}$  symmetry, C-C = 1.392  $\text{\AA}$ ), and with the remaining atoms as individual isotropic atoms, resulted in agreement factors of  $R_1 = \sum(|F_o| - |F_c|)/\sum|F_o| = 0.072$  and  $R_2 = (\sum w(|F_o| - |F_c|)^2/\sum w(F_o^2))^{1/2} = 0.102$ .

Positional and thermal parameters for the 28 hydrogen atoms in the molecule were calculated by assuming a C-H distance of 0.95  $\text{\AA}$ , regular  $C_{6v}^2$  geometry, and isotropic thermal parameters 1.0  $\text{\AA}^2$  greater than the carbon to which each is bonded. These "ideal" positions all agreed well with positive peaks in a difference Fourier synthesis; hence the contributions from the H atoms were included in subsequent refinement cycles, although no attempt was made to refine their positional or thermal parameters.

One cycle of refinement, followed by recalculation of the H atom parameters, followed by two further refinement cycles, served to converge the model to final agreement factors of  $R_1 = 0.047$  and  $R_2 = 0.064$ . In the final cycles, 283 variables were refined by using 5096

observations, and no parameter shift exceeded 0.57 times its estimated standard deviation. The error in an observation of unit weight is 1.690 e. In a difference Fourier calculated from the final structure factors, the 20 highest peaks, ranging from 0.6 to 1.9 e  $\text{\AA}^{-3}$ , are associated with the four phenyl rings and arise as a result of constraining them to behave as rigid groups. A statistical analysis of  $R_2$  in terms of  $|F_o|$ ,  $\lambda^{-1} \sin \theta$ , and various combinations of Miller indices, showed no significant trends.

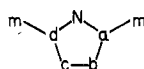
The individual atomic positional and thermal parameters are given in Table II, and the rigid group parameters are listed in Table III. The derived H atom parameters are presented in Table IV, and Table V lists the final calculated and observed structure factor amplitudes.<sup>7</sup>

- (7) Supplementary material.
- (8) R. D. Shannon and C. T. Prewitt, *Acta Crystallogr. Sect. B*, **26**, 1076 (1970).
- (9) A. Fitzgerald, private communication.
- (10) J. L. Hoard, N. Kim, and J. W. Buchler, "Abstracts of Papers", 167th National Meeting of the American Chemical Society, Los Angeles, Ca, 1974; American Chemical Society, Washington, DC, INOR 75.
- (11) K. Henrick, R. W. Matthews, and P. A. Tasker, *Inorg. Chem.*, **16**, 3293-8 (1977).
- (12) W. Bolton and M. F. Perutz, *Nature (London)*, **228**, 551 (1970).
- (13) D. L. Cullen, E. F. Meyer, Jr., and K. M. Smith, *Inorg. Chem.*, **16**, 1179-87 (1977).
- (14) G. Fermi, *J. Mol. Biol.*, **97**, 237-56 (1975).
- (15) F. Molinaro and J. A. Ibers, *Inorg. Chem.*, **15**, 2278-83 (1976).
- (16) B. Gonzales, J. Kouba, S. Yee, C. A. Reed, J. F. Kirner, and W. R. Scheidt, *J. Am. Chem. Soc.*, **97**, 3247-9 (1975).

(6) (a) "International Tables for X-ray Crystallography", Vol. IV, Kynoch Press, Birmingham, England, 1972, p 99. (b) D. T. Cromer and D. Liberman, *J. Chem. Phys.*, **53**, 1891 (1970).

Table VI. Selected Interatomic Distances (Å) and Angles (Deg)

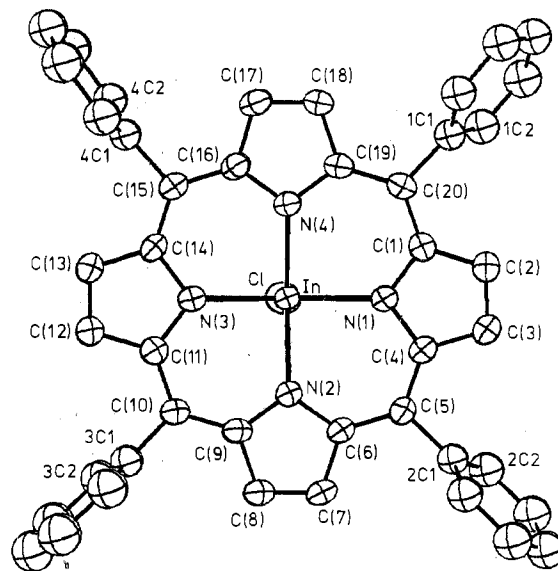
Distances							
In-N(1)	2.160 (4)	N(2)-C(9)	1.380 (6)	C(6)-C(7)	1.430 (7)	C(16)-C(17)	1.437 (7)
In-N(2)	2.158 (4)	N(3)-C(11)	1.380 (6)	C(7)-C(8)	1.344 (7)	C(17)-C(18)	1.344 (7)
In-N(3)	2.158 (4)	N(3)-C(14)	1.378 (6)	C(8)-C(9)	1.431 (6)	C(18)-C(19)	1.437 (6)
In-N(4)	2.146 (4)	N(4)-C(16)	1.377 (6)	C(9)-C(10)	1.399 (7)	C(19)-C(20)	1.412 (7)
In-Cl	2.369 (2)	N(4)-C(19)	1.372 (6)	C(10)-C(11)	1.403 (7)	C(20)-C(1)	1.393 (7)
N(1)-N(3)	4.150 (6)	C(1)-C(2)	1.434 (7)	C(11)-C(12)	1.438 (7)	C(20)-1C1	1.506 (6)
N(2)-N(4)	4.118 (5)	C(2)-C(3)	1.349 (7)	C(12)-C(13)	1.354 (7)	C(5)-2C1	1.498 (6)
N(1)-C(1)	1.386 (6)	C(3)-C(4)	1.428 (7)	C(13)-C(14)	1.436 (7)	C(10)-3C1	1.502 (7)
N(1)-C(4)	1.383 (6)	C(4)-C(5)	1.411 (7)	C(14)-C(15)	1.394 (7)	C(15)-4C1	1.507 (6)
N(2)-C(6)	1.378 (6)	C(5)-C(6)	1.400 (7)	C(15)-C(16)	1.403 (7)		
Angles							
N(1)-In-N(2)	85.5 (2)	In-N(3)-C(14)	125.9 (3)	N(3)-C(11)-C(12)	109.0 (4)	C(5)-C(6)-C(7)	125.6 (4)
N(2)-In-N(3)	85.2 (1)	In-N(4)-C(16)	125.4 (3)	N(3)-C(14)-C(13)	108.8 (4)	C(6)-C(7)-C(8)	107.7 (4)
N(3)-In-N(4)	85.4 (2)	In-N(4)-C(19)	125.6 (3)	N(4)-C(16)-C(17)	108.6 (4)	C(7)-C(8)-C(9)	108.2 (5)
N(4)-In-N(1)	85.5 (2)	N(1)-C(1)-C(20)	125.7 (4)	N(4)-C(19)-C(18)	108.8 (4)	C(8)-C(9)-C(10)	126.1 (5)
N(1)-In-N(3)	147.9 (2)	N(1)-C(4)-C(5)	124.7 (5)	1C1-C(20)-C(19)	115.5 (2)	C(9)-C(10)-C(11)	126.2 (5)
N(2)-In-N(4)	146.3 (2)	N(2)-C(6)-C(5)	125.9 (4)	1C1-C(20)-C(1)	118.4 (2)	C(10)-C(11)-C(12)	125.4 (5)
Cl-In-N(1)	105.1 (1)	N(2)-C(9)-C(10)	125.9 (4)	2C1-C(5)-C(4)	116.1 (2)	C(11)-C(12)-C(13)	107.2 (5)
Cl-In-N(2)	105.9 (1)	N(3)-C(11)-C(10)	125.5 (4)	2C1-C(5)-C(6)	117.0 (2)	C(12)-C(13)-C(14)	107.8 (4)
Cl-In-N(3)	106.9 (1)	N(3)-C(14)-C(15)	125.5 (4)	3C1-C(10)-C(9)	116.3 (2)	C(13)-C(14)-C(15)	125.6 (4)
Cl-In-N(4)	107.8 (1)	N(4)-C(16)-C(15)	126.2 (4)	3C1-C(10)-C(11)	117.4 (3)	C(14)-C(15)-C(16)	126.0 (4)
In-N(1)-C(1)	125.9 (3)	N(4)-C(19)-C(20)	125.8 (4)	4C1-C(15)-C(14)	118.8 (2)	C(15)-C(16)-C(17)	125.1 (4)
In-N(1)-C(4)	126.4 (3)	N(1)-C(1)-C(2)	108.2 (4)	4C1-C(15)-C(16)	115.0 (2)	C(16)-C(17)-C(18)	107.6 (4)
In-N(2)-C(6)	125.1 (3)	N(1)-C(4)-C(3)	108.9 (4)	C(1)-C(2)-C(3)	108.1 (5)	C(17)-C(18)-C(19)	107.6 (4)
In-N(2)-C(9)	124.7 (3)	N(2)-C(6)-C(7)	108.4 (4)	C(2)-C(3)-C(4)	107.6 (4)	C(18)-C(19)-C(20)	125.2 (4)
In-N(3)-C(11)	125.6 (3)	N(2)-C(9)-C(8)	108.0 (4)	C(3)-C(4)-C(5)	126.2 (4)	C(19)-C(20)-C(1)	126.0 (4)
				C(4)-C(5)-C(6)	126.7 (4)	C(20)-C(1)-C(2)	126.0 (5)



	pyrrole 1	pyrrole 2	pyrrole 3	pyrrole 4	av
N-a	1.386 (6)	1.377 (6)	1.380 (6)	1.378 (6)	1.380 (4)
N-d	1.383 (6)	1.378 (6)	1.378 (6)	1.380 (6)	1.380 (2)
a-b	1.434 (7)	1.437 (6)	1.438 (7)	1.430 (7)	1.435 (4)
b-c	1.349 (6)	1.344 (7)	1.354 (7)	1.344 (7)	1.348 (5)
c-d	1.428 (6)	1.437 (7)	1.436 (7)	1.431 (6)	1.433 (4)
a-m	1.393 (7)	1.403 (7)	1.403 (7)	1.400 (7)	1.402 (7)
d-m	1.411 (7)	1.412 (7)	1.394 (7)	1.399 (7)	
a-N-d	107.1 (4)	107.3 (1)	107.2 (4)	107.7 (4)	107.3 (3)
N-a-b	108.2 (4)	108.6 (4)	109.0 (4)	108.4 (4)	108.5 (3)
N-d-c	108.9 (4)	108.8 (4)	108.8 (4)	108.0 (4)	108.6 (4)
a-b-c	108.1 (5)	107.6 (4)	107.2 (5)	107.7 (4)	107.6 (4)
b-c-d	107.6 (4)	107.6 (4)	107.8 (4)	108.2 (5)	107.8 (3)

Table VI lists selected interatomic distances and angles and Table VII gives the equation and perpendicular displacements from two

- (17) A. B. Hoffman, D. M. Collins, V. W. Day, E. B. Fleischer, T. S. Srivastava, and J. L. Hoard, *J. Am. Chem. Soc.*, **94**, 3620-6 (1972).
- (18) D. F. Koenig, *Acta Crystallogr.*, **18**, 663 (1965).
- (19) J. L. Hoard and W. R. Scheidt, *Proc. Natl. Acad. Sci. U.S.A.*, **70**, 3919 (1973); **71**, 1578 (1974).
- (20) T. Takano, *J. Mol. Biol.*, **110**, 569-84 (1977).
- (21) G. B. Jameson, F. Molinaro, J. A. Ibers, J. P. Collman, J. I. Brauman, E. Rose, and K. S. Suslick, *J. Am. Chem. Soc.*, **100**, 6769-70 (1978).
- (22) H.-C. Chow, R. Serlin, and C. E. Strouse, *J. Am. Chem. Soc.*, **97**, 7230-6 (1975).
- (23) R. Serlin, H.-C. Chow, and C. E. Strouse, *J. Am. Chem. Soc.*, **97**, 7237-42 (1975).
- (24) J. L. Hoard, G. H. Cohen, and M. D. Glick, *J. Am. Chem. Soc.*, **89**, 1992-6 (1967).
- (25) D. M. Collins and J. L. Hoard, *J. Am. Chem. Soc.*, **92**, 3761-71 (1970).
- (26) D. L. Cullen and E. F. Meyer, Jr., *Acta Crystallogr., Sect. B*, **32**, 2259-69 (1976).
- (27) M. F. Perutz, *Nature (London)*, **228**, 726-34 (1970).
- (28) R. Huber, O. Epp, and H. Formanek, *J. Mol. Biol.*, **52**, 349-54 (1970).
- (29) T. Takano, *J. Mol. Biol.*, **110**, 537-68 (1977).
- (30) B. M. Chen, Ph.D. Thesis, Michigan State University, 1970.
- (31) R. Timkovich and A. Tulinsky, *J. Am. Chem. Soc.*, **91**, 4430 (1969).
- (32) V. W. Day, B. R. Stults, E. L. Tasset, R. S. Marianelli, and L. J. Boucher, *Inorg. Nucl. Chem. Lett.*, **11**, 505-9 (1975).
- (33) S. E. V. Phillips *Nature (London)*, **273**, 247-8 (1978).
- (34) V. W. Day, B. R. Stults, E. L. Tasset, R. S. Marinelli, and L. J. Boucher, *Inorg. Nucl. Chem. Lett.*, **11**, 505-9 (1975).
- (35) R. G. Little and J. A. Ibers, *J. Am. Chem. Soc.*, **96**, 4452-63 (1974).
- (36) W. R. Scheidt, *J. Am. Chem. Soc.*, **96**, 90-4 (1974).

Figure 1. Atomic numbering system for crystalline InTPPCl. The atoms are drawn as 50% probability thermal ellipsoids. The H atoms have been omitted for clarity. The phenyl rings are numbered as  $nCm$ , where  $n$  is the group number ( $n = 1-4$ ) and  $m$  is the ring carbon ( $m = 1-6$ ).

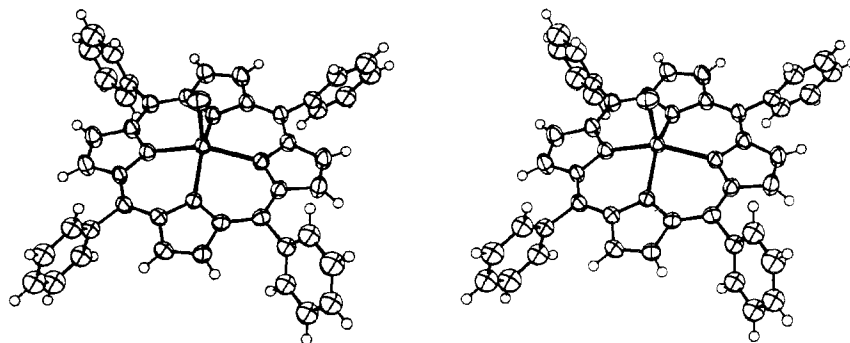


**Figure 2.** Stereo diagram of InTPPCl, illustrating the In displacement from the macrocyclic plane and the "doming" of the porphyrin skeleton. The H atoms have been arbitrarily reduced for clarity.

**Table VII.** Selected Planes of the Porphyrin Macrocyclic Skeleton (See Text)

Planes

plane 1:  $-9.0724x + 6.6598y + 3.3759z + 2.0712 = 0^a$   
 plane 2:  $-9.1418x + 6.4518y + 3.2405z + 2.2543 = 0$

Perpendicular Displacements<sup>b</sup> (Å)

Plane 1			
In	0.6104 (3)	C(10)	-0.052 (5)
Cl	2.978 (2)	C(11)	-0.049 (5)
N(1)*	-0.014 (4)	C(12)	-0.185 (6)
N(2)*	-0.014 (4)	C(13)	-0.224 (6)
N(3)*	0.015 (4)	C(14)	-0.086 (5)
N(4)*	-0.014 (4)	C(15)	-0.122 (5)
C(1)	-0.136 (5)	C(16)	-0.095 (5)
C(2)	-0.347 (6)	C(17)	-0.219 (6)
C(3)	-0.356 (6)	C(18)	-0.204 (5)
C(4)	-0.117 (5)	C(19)	-0.089 (5)
C(5)	-0.128 (5)	C(20)	-0.141 (5)
C(6)	-0.074 (5)	1C1	-0.241 (3)
C(7)	-0.103 (6)	2C1	-0.327 (3)
C(8)	-0.068 (6)	3C1	-0.163 (3)
C(9)	-0.029 (5)	4C1	-0.310 (3)

Plane 2			
In	0.7115 (3)	C(10)*	-0.006 (5)
Cl	3.079 (2)	C(11)*	0.006 (5)
N(1)*	0.141 (4)	C(12)*	-0.142 (6)
N(2)*	0.066 (4)	C(13)*	-0.168 (6)
N(3)*	0.091 (4)	C(14)*	-0.008 (5)
N(4)*	0.108 (4)	C(15)*	-0.025 (5)
C(1)*	0.012 (5)	C(16)*	0.023 (5)
C(2)*	-0.187 (6)	C(17)*	-0.082 (6)
C(3)*	-0.211 (6)	C(18)*	-0.051 (6)
C(4)*	0.007 (5)	C(19)*	0.055 (5)
C(5)*	-0.023 (3)	C(20)*	0.015 (5)
C(6)*	0.011 (5)	1C1	-0.061 (3)
C(7)*	-0.038 (6)	2C1	-0.220 (4)
C(8)*	-0.019 (6)	3C1	-0.141 (4)
C(9)*	0.028 (5)	4C1	-0.214 (4)

<sup>a</sup> The plane equations are in terms of crystal coordinates. <sup>b</sup> Asterisk indicates the atoms included in the calculation of the mean plane.

possible mean planes through the porphyrin core.

## Results and Discussion.

The atomic numbering system for InTPPCl is shown in Figure 1, and a stereo drawing of InTPPCl is shown in Figure 2. The displacement of the indium atom above the mean plane of the four pyrrole nitrogen atoms is clearly evident in Figure 2, as is the measurable "doming" of the macrocyclic skeleton.

The significant features of the InTPPCl structure are most evident from comparison of the InTPPCl parameters with those of other metalloporphyrins exhibiting measurable displacement of the metal ion above the mean pyrrole nitrogen plane, as summarized in Table VIII. The entries in Table

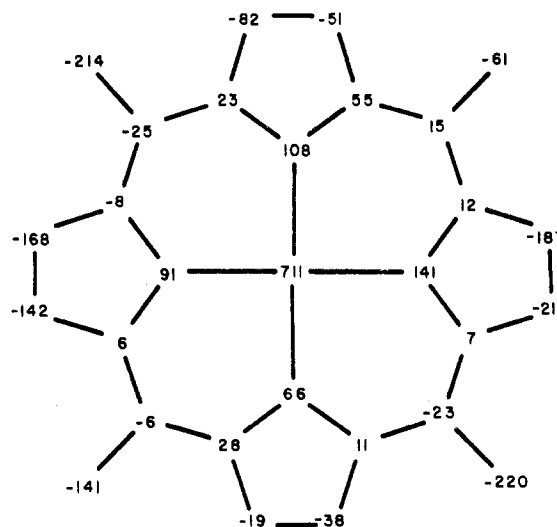


**Figure 3.** Atomic displacements ( $\text{\AA} \times 10^3$ ) from the mean porphyrin plane (plane 2 of Table VII) of InTPPCl. Positive numbers correspond to displacements toward the indium atom.

VIII have been ordered according to the displacement of the metal atom above the mean pyrrole nitrogen plane.

**Metal Displacement above the Mean Pyrrole Nitrogen Plane.** Three features of the metal displacement are apparent from Table VIII: (1) there is no simple correlation between ionic radius and metal ion displacement; (2) the displacements for the *same* metal coordinated to *different* porphyrins are similar (cf. the Zn(II) entries in Table VIII); and (3) indium(III) is displaced by essentially the same distance as is Fe(II) in deoxyhemoglobin (horse or human). (An exception to observation (2) is the recent characterization of high-spin Fe(III) complexes with the iron atom precisely *in* the mean porphyrin plane.<sup>37</sup>) Observation (2) lends generality to any new metal metalloporphyrin structure with a new metal atom. In the present case, we can thus predict with some confidence that any subsequent five-coordinate indium porphyrin complexes will exhibit similar indium displacement above the mean porphyrin plane.

It is interesting to note that although Co(II) has the same ionic radius as high-spin Fe(III), the Fe(III) is displaced farther above the mean porphyrin plane by some 0.3 Å. Moreover, it is known that CoHb exhibits oxygen-binding cooperativity, although to a lesser degree than native Hb.<sup>38</sup> Since the allosteric Perutz mechanism for hemoglobin cooperativity depends directly upon the large (ca. 0.6 Å) change

(37) T. Mashiko, M. E. Kastner, K. Spartalian, W. R. Scheidt, and C. A. Reed, *J. Am. Chem. Soc.*, **100**, 6354-62 (1978).

(38) K. Imai, T. Yonetani, and M. Ikeda-Saito, *J. Mol. Biol.*, **109**, 83 (1977); H. A. Saroff and A. P. Minton, *Science*, **175**, 1253 (1972).

Table VIII. Representative Metalloporphyrins with Significant Out-of-Plane Metal Ion Displacement<sup>a</sup>

metal	oxidation state	ionic radius, <sup>b</sup> Å	metalloporphyrin	coordin. no.	metal ion displacement, <sup>c</sup> Å	(M-N) <sub>av</sub> , Å	core radius, <sup>d</sup> Å	doming, <sup>e</sup> Å	ref
Bi	III	0.99	Bi(OEP) <sup>+</sup>	5	1.09	2.32	2.047	0.13	9
Zr	IV	0.84	(OAc) <sub>2</sub> Zr(OEP)	8	1.02	2.268, 2.259	2.024, 2.014	0.17, 0.21	10
Hf	IV	0.83	(OAc) <sub>2</sub> Hf(OEP)	8	1.01	2.257	2.016	0.13	10
Tl	III	0.88	CH <sub>3</sub> Tl(TPP)	5	0.98	2.291	2.071	0.10	11
Fe	II	0.78	deoxyhemoglobin (horse)	(6)	0.75 <sup>f</sup>				12
Tl	III	0.88	ClTl(TPP)	5	0.74	2.210	2.083	0.09	11
Tl	III	0.88	ClTl(OEP)	5	0.69	2.212	2.10	0.06	13
In	III	0.80	ClIn(TPP)	5	0.61	2.156	2.067	0.10	13
Fe	II	0.78	deoxyhemoglobin (human)	(6)	0.63 (β) <sup>f</sup>	2.1	2.00 <sup>g</sup>	0.22 (α); 0.17 (β)	14
(VO)	(IV)	(0.64)	OV(OEP)	4	0.54	2.101	2.030	0.06	15
Mn	II	0.82	(1-MeIm) <sub>2</sub> Mn(TPP)	5	0.52	2.128	2.065	0.04	16
Fe	III	0.65	O[Fe(TPP)] <sub>2</sub>	5	0.50	2.087	2.027	0.04	17
Fe	III	0.65	ClFe(proto-IX)	5	0.48	2.062	2.007	0.06	18
Fe	II	0.78	(2-MeIm)Fe(TPP)	5	0.42	2.086	2.044	0.13	19
Fe	II	0.78	deoxymyoglobin (sperm whale)	(6)	0.42	2.06	2.033	0.13	20
Fe	II	0.78	(2-MeIm)Fe(TpivPP)	5	0.40	2.072		0.03	21
Mg	II	0.72	ethyl chlorophyllide <sup>a</sup>	5	0.39	2.086		0.04 <sup>h</sup>	22
Mg	II	0.72	ethyl chlorophyllide <sup>b</sup>	5	0.39	2.081		0.01 <sup>h</sup>	23
Fe	III	0.65	ClFe(TPP)	5	0.38 <sup>i</sup>	2.049			24
Zn	II	0.68	(ClO) <sub>2</sub> Zn(TPP)	5	0.35	2.076	2.046	0.09	25
Zn	II	0.68	(py)Zn(TpyP)	5	0.33	2.073	2.047	0.04	26
Zn	II	0.68	(py)Zn(OEP)	5	0.31	2.067	2.043	0.09	27
Fe	III	0.65	methemoglobin (horse)	(6)	~0.3 <sup>f</sup>				28
Fe	III	0.78	deoxyerythrocyrin	(6)	~0.3 <sup>f</sup>				29
Fe	III	0.65	metmyoglobin (whale)	(6)	0.27	2.04	2.00 <sup>g</sup>	0.13	30
Mn	III	0.58	ClMn(TPP)	5	0.27	2.008	1.989	0.0	31
Mg	II	0.82	(H <sub>2</sub> O)Mg(TPP)	5	0.27 <sup>i</sup>	2.072	2.055		32
Fe	II	0.61	oxymyoglobin (whale)	(6)	0.26				33
Mn	III	0.58	(N <sub>3</sub> )Mn(TPP)	5	0.23	2.005	1.992		34
Co	II	0.65	(1-MeIm)Co(OEP)	5	0.13	1.955	1.950	0.03	35
Co	II	0.65	(1-MeIm)Co(TPP)	5	0.13	1.977	1.973	0.01	36

<sup>a</sup> Abbreviations: OAc, acetate; Me, methyl; py, pyridine; OEP, octaethylporphyrin dianion; TPP, tetraphenylporphyrin dianion; proto-IX, protoporphyrin IX dianion; TpyP, tetrakis(4-pyridyl)porphyrin dianion; TpivPP, *meso*-5,10,15,20-tetrakis(*o*-pivalamidophenyl)porphyrinato. <sup>b</sup> From ref 8. <sup>c</sup> Perpendicular displacement of the metal ion from the mean plane of the four pyrrole nitrogens. <sup>d</sup> Average distance from the center of the plane of the four pyrrole nitrogens to a pyrrole nitrogen. <sup>e</sup> Difference between the displacement of the metal from the mean plane of the four pyrrole nitrogens and the mean plane of the 24-atom porphyrin skeleton. <sup>f</sup> Displacement in this case is measured from the mean plane of the 24-atom porphyrin skeleton. <sup>g</sup> This distance was constrained to this value in refining the atomic positions. <sup>h</sup> Average distance from the N<sub>1</sub>-N<sub>2</sub>-N<sub>3</sub> plane. <sup>i</sup> Estimated (disordered structure).

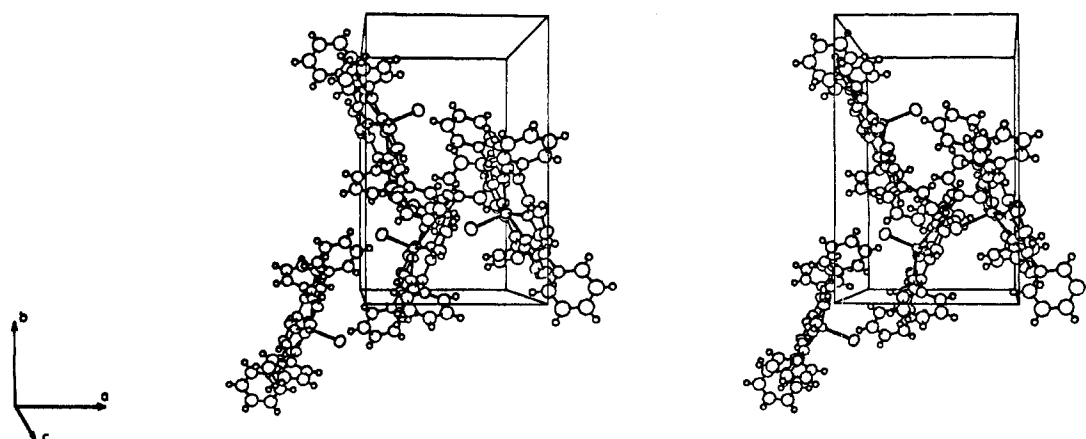


Figure 4. Stereoscopic view of the contents of one unit cell of crystalline InTPPCl.

in Fe(II) displacement above the porphyrin plane upon oxygen binding,<sup>2</sup> it is logical to wonder whether or not the Perutz "trigger" mechanism is consistent with the much smaller out-of-plane displacement of Co(II) in model metalloporphyrins. The most reasonable rationalization of this dilemma is that of Hoard and Scheidt<sup>19</sup> and Little and Ibers,<sup>35</sup> who propose that the porphyrin skeleton is severely deformed by upward "doming" (ca. 0.3 Å) toward the cobalt atom in CoHb. CoHb is therefore thought to achieve the "tense" quarternary structure, not so much by the separation between the Co(II) and the mean porphyrin plane but rather by marked distortion of the porphyrin skeleton itself to move the cobalt nearer to the proximal histidine in the active site.

Since the "relaxed" quarternary structures of CoHb and Hb (e.g., after oxygen-binding, so that the metal atom lies in the porphyrin plane) are expected to be similar, while the overall functional properties are so different (e.g., oxygen affinity reduced by 10–100 times for CoMb and CoHb compared to Mb and Hb;<sup>39</sup> free energy difference between intrinsic binding of the first and fourth O<sub>2</sub> to CoHb reduced to one-third that of Hb<sup>38</sup>), it seems reasonable to conclude that the "tense" quarternary structures of CoHb and Hb must be appreciably different, most probably because of the much smaller displacement of Co above the porphyrin plane. In seeking a metalloporphyrin which, when reconstituted into apohemoglobin, will produce a "tense" conformation more similar to that for the native iron-containing protein, one therefore seeks a case for which the metal displacement above the porphyrin plane is more similar to that for the corresponding high-spin Fe(II) complex.

From Table VIII, it is clear that there are relatively few attractive candidates. MnHb has been prepared<sup>40</sup> but is irreversibly oxidized to Mn<sup>III</sup>Hb. Mg and Zn,<sup>41</sup> while presumably stable toward oxidation, exhibit relatively small metal displacement above the porphyrin plane and may thus not be appreciably better than Co in this respect. The large ions, Tl, Hf, Zr, and Bi, give displacements which may be too large (compared to Fe), and in the cases of Hf and Zr give unsuitable coordination number. However, the present results suggest that an indium porphyrin may be an ideal candidate for inducing the "tense" conformation in hemoglobin, without the complication of oxygen binding to the indium-labeled subunits and with near-ideal displacement of the metal ion from the mean porphyrin plane. We have in fact already reconstituted indium mesoporphyrin IX into apomyo-

globin and have used  $\gamma$ - $\gamma$  angular correlations to determine the rotational correlation time for the central metal atom.<sup>42</sup> Extension to hemoglobin is in progress. It should prove especially interesting to reconstitute "hybrid" hemoglobins, in which half the subunits (say the  $\alpha$  units) are reconstituted with indium and the other half with iron. Then it will be possible to monitor oxygen binding to, say, the  $\beta$  subunits, with the  $\alpha$  subunits "frozen" into the "tense" conformation.

**Bond Lengths and Angles.** The bond lengths and angles of Table VI show that the square-pyramidal InTPPCl molecule has very close to  $C_{4v}$  symmetry, as far as the In, Cl, and porphyrin skeleton atoms are concerned. (The phenyl tilts are discussed below.) The average In–N distance is 2.156 (6) Å, which is substantially larger than for the corresponding high-spin Fe(III) complexes (ca. 2.05–2.09 Å). This increase is due partly to expansion of the porphyrin core (radius of 2.067 Å for InTPPCl, compared to approximately 2.00–2.04 Å for iron(III)) and partly to an intrinsically longer In–N bond compared to Fe–N bond. However, the Fe–N bond length for iron in hemoglobin is expected to increase to approximately the present In–N value, due to tension produced by the proximal histidine ligand of Hb;<sup>19,35</sup> thus the indium porphyrin may still be a close structural analogue for Fe(II) in deoxyhemoglobin, even though the isolated porphyrin structures appear rather different with respect to metal–nitrogen bond lengths.

**Doming of the Porphyrin Skeleton.** Hoard<sup>43</sup> and co-workers have demonstrated the high degree of flexibility of the porphyrin skeleton in metalloporphyrin crystal structures. InTPPCl exhibits marked deviations from planarity of the porphyrin atoms, as shown by the displacements illustrated in Figure 3. The perpendicular displacements (in Å  $\times 10^3$ , where positive and negative values correspond to displacements above (i.e., toward the indium) or below the plane) from the mean plane of all 24 core porphyrin atoms in Figure 3 show that the porphyrin skeleton is appreciably "domed" upward toward the indium. The plane of the four pyrrole nitrogens is in fact displaced some 0.10 Å above the mean plane of the core porphyrin atoms, and the outermost pyrrole ring carbons are depressed by up to 0.211 Å below the plane. This degree of doming is well within the range observed for high-spin ferric porphyrins (Table VIII) and suggests that the porphyrin skeleton is not unusually distorted by the presence of the indium atom.

**Phenyl Rings: Crystal Packing.** A stereoview of a unit cell is shown in Figure 4 and illustrates the molecular packing. The closest nonbonded intermolecular contact is 2.48 Å between

(39) C. A. Spillburg, B. M. Hoffman, and D. H. Petering, *J. Biol. Chem.*, **247**, 4219 (1972).

(40) C. Bull, R. G. Fisher, and B. M. Hoffman, *Biochim. Biophys. Res. Commun.*, **59**, 140 (1974).

(41) J. J. Leonard, T. Yonetani, and J. B. Callis, *Biochemistry*, **13**, 1460–4 (1974).

(42) A. G. Marshall, K. M. Lee, and P. W. Martin, *J. Am. Chem. Soc.*, **102**, 1450 (1980).

(43) J. L. Hoard, *Science*, **174**, 1295–302 (1971).

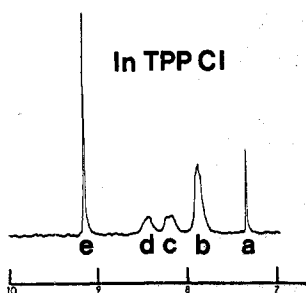


**Figure 5.**  $^1\text{H}$  100-MHz FT-NMR spectrum of InTPPCl in  $\text{CDCl}_3$  solvent. Peak assignments are as follows: (a) residual  $\text{CHCl}_3$  ( $\delta = 7.33$ ); (b) meta and para phenyl protons (7.87); (c) and (d) ortho phenyl protons (8.20 and 8.43); and (e) pyrrole  $\beta$ -protons (9.15). Spectrum was obtained by using a Varian XL-100 FT-NMR spectrometer, with  $\text{CDCl}_3$  used for  $^2\text{D}$  lock, 10 transients, 6.0-s pulse delay, and sensitivity enhancement time constant of  $-1.0$  s.

$\text{H4C4}$  and  $\text{H3C3}$  at  $(1-x, 1-y, z)$ , indicating that there is no strong hydrogen bonding network and only the normal van der Waals forces between molecules.

It is of interest to note that phenyl ring 1 is twisted by only  $66.17^\circ$  with respect to the mean porphyrin skeletal plane, while the other three rings have dihedral angles that are closer to perpendicular ( $107.59$ ,  $93.67$ , and  $98.33^\circ$  for phenyl rings 2-4, respectively).

That the four phenyl rings are equivalent in solution is shown by the proton NMR spectrum of InTPPCl in Figure 5. When this spectrum was first observed,<sup>3</sup> the magnetically inequivalent ortho protons of the phenyl rings were incorrectly ascribed to "nonequivalence of phenyls in pairs", presumably due to two chemically different sets of two phenyls each. The present crystal structure indicates that the inequivalence arises from the displacement of the indium above the porphyrin ring, making the upper (four) and lower (four) ortho protons in-

equivalent. The coalescence of these two ortho proton peaks on increase in temperature<sup>44,45</sup> thus arises from internal rotation of the chemically equivalent phenyl groups about the bonds which connect the phenyl rings to the porphyrin skeleton. Such a mechanism was proposed even before the crystal structures were known, for the related thallium(III) porphyrins.<sup>45</sup>

#### Summary

On the basis of the high degree of analogy between the principal structural features of InTPPCl compared to iron(III) porphyrins and iron(II) deoxyhemoglobin (e.g., displacement of metal atom above the mean porphyrin plane, distance from metal to pyrrole nitrogen, porphyrin core expansion, doming of porphyrin skeletal core atoms), it is suggested that reconstitution of an indium porphyrin into apohemoglobin should produce the quarternary "tense" conformation. The relatively large tilt angle for one of the four phenyl groups of InTPPCl with respect to the mean porphyrin plane is explained in terms of crystal packing effects, and the phenyl groups are shown by NMR to be equivalent in solution.

**Acknowledgment.** The authors wish to thank Professor A. W. Addison of Drexel University and Professors D. Dolphin, B. R. James, and A. Storr of the University of British Columbia for helpful comments and discussions.

**Registry No.** InTPPCl, 63128-70-1.

**Supplementary Material Available:** Tables IV and V (derived H atom positions; calculated and observed structure factor amplitudes) (69 pages). Ordering information is given on any current masthead page.

(44) S. S. Eaton and G. R. Eaton, *J. Am. Chem. Soc.*, **99**, 6594-9 (1977).

(45) R. J. Abraham, G. H. Barnett, and K. M. Smith, *J. Chem. Soc., Perkin Trans.*, 2142-8 (1973).